Reducing Orbit Error for a Better Estimate of Oceanic Variability from Satellite Altimetry

F. BLANC

CLS ARGOS Toulouse, France

P. Y. LE TRAON

CLS ARGOS Toulouse, France

S. HOURY

GRGS/UMR39 Toulouse, France

(Manuscript received 25 January 1993, in final form 2 January 1994)

ABSTRACT

The variable ocean dynamic topography is generally estimated from the satellite altimeter signal once the orbit error has been removed. To compute the orbit error, the most conventional technique is to fit a polynomial function (zeroth, first, or second degree) over lengths of several thousand kilometers to each altimetric profile. However, the method induces significant errors. To reduce them, one needs a more detailed representation of the orbit error spectrum and to take account of the spatial and temporal characteristics of the signal and noise. This can be achieved by the form of optimal analysis known as "inverse theory." If a realistic statistical description of the altimeter signal components (i.e., oceanic variability and orbit error) is provided, the inverse formalism optimally separates the components. Although the whole set of altimeter data is reduced to the data at the intersections of ascending and descending ground tracks (crossover points), the method remains quasi-optimal.

The authors highlight the effectiveness of the method by applying it to the altimeter data for the Brazil–Malvinas confluence area, a few thousand kilometers wide. The authors compare the orbit error estimates to those of the most conventional method that is a method set to a similar environment (short-arc analyses). With a homogeneous oceanic variability of 15 cm rms and a nominal orbit error of 30 cm rms, the error on the estimation is reduced to 2 cm all along the altimetric profiles. Taking into account the nonhomogeneous characteristics of the variability signal improves the estimation. It can be further improved simply by adding to the selected altimeter dataset the crossover points one orbital revolution away. For the Geosat satellite, they are at the same latitude but 25°25′ farther west or east. The results encourage the use of the inverse method for orbit error reduction. The method is good at separating signals once the a priori parameters are well defined. Unlike polynomial fits, it does not remove other residual environmental terms.

1. Introduction

Satellite altimeter missions give oceanographers the opportunity to study the sea level variations with a high spatial and temporal resolution (Douglas et al. 1987). From the successful *GEOS-3,* Seasat, and Geosat missions, basic tools for extracting the sea surface variability signal from altimeter data have been established and refined. A major remaining difficulty is how to correct the uncertainty in the estimation of satellite altitude, the so-called radial orbit error.

A widely used method to correct for orbit error and estimate the variable oceanic signal in local areas is collinear-track analysis (Cheney et al. 1983; Ménard 1983): altimeter profiles obtained along identical ground tracks are referred to the "mean one." The residual orbit error is a long wavelength signal: orbital analyses have shown that its frequency spectrum is characterized by a prominent peak at the once per orbital revolution frequency (i.e., a wavelength of about 40 000 km) so that at scales under a few thousand kilometers it has often been approximated by a low-degree polynomial or sinusoid (Tai 1989). The most conventional orbit error removal procedure adjusts low-degree polynomials (degrees 0, 1, or 2) independently for each profile, to distances of a few thousand kilometers (short-arc analyses). But the procedure attenuates the oceanic signal and can induce significant errors (Sandwell and Zangh 1989; Cheney and Miller 1990) since there are insufficient independent data (degrees of freedom) to constrain estimation of the polynomial satisfactorily. The adjustment acts like a high-pass filter, and scales comparable to or larger than the region are treated as orbit error and removed accordingly (Cheney et al. 1989). This effect was inves-

Corresponding author address: Frederique Blanc, Collecte Localisation Satellites, 18 Avenue Edouard-Belin, 31055 Toulouse, Cedex, France.

tigated theoretically by Le Traon et al. (1991). It depends, of course, on the spatial and energetic characteristics of the oceanic signal (variability level, nonhomogeneities). For a first-degree adjustment over 1500 km or a second-degree adjustment over 2500 km, Le Traon et al. show that its amplitude is typically 30% of the total signal amplitude at the profile center, reaching 50% at the ends. And it can be greater than the total signal amplitude when there are strong nonhomogeneities. These errors directly impact the mapping of the oceanic variable circulation. To preserve more of the oceanic signal, the track segments can be lengthened to profiles of half or a few revolutions and adjusted with sinusoids (Chelton et al. 1990; Wagner et al. 1992). The orbit error removal procedure then behaves as a band-elimination filter rather than a high-pass filter. It still affects the oceanic signal but on a global scale (e.g., seasonal heating) (Tai 1991; Van Gysen et al. 1992). The weakness of adjustment methods is that they do not take account of the difference in time correlation between the orbit error and the oceanic signal.

Another method called the "crossover-difference approach" uses altimeter measurements at intersections of ascending and descending ground tracks to remove the mean oceanic signal (Marsh and Martin 1982; Fu and Chelton 1985; Tai and Fu 1986). The variable signal is then separated from the residual orbit error signal by adjusting linear trends or sine waves to minimize the residual crossover differences. However, the solution to the least-squares problem is not unique: the region as a whole can be lifted or lowered, tilted one way or another. The method needs at least one defined reference arc, or other constraints, to estimate the eddy field variability. Tai (1988) has been particularly careful on the constraint to introduce. He parameterizes the radial orbit error for each satellite orbital revolution as a sine wave of wavelength equaling once per revolution. The uncertainty characterizing crossover adjustment methods is solved by minimizing the coefficients to be determined and the crossover differences. But this method is still not optimal, because, it does not take account of the temporal correlation of orbit error for different tracks, nor is it based on a complete statistical description of the altimeter signal.

The oceanic variability is estimated from altimetry once the oceanic signal and error components are separated out. This can be done using the form of optimal analysis known as inverse theory (Tarantola and Valette 1982; Wunsch and Zlotnicki 1984; Mazzega and Houry 1989). Given the uncertainties in our knowledge of the gravitational field, we first used the collinear approach to remove its influence on the mean sea surface and orbit determinations. This leaves a set of altimeter residuals that reveal both the variability signal and the residual orbit error. If we now provide a realistic statistical description of those two signals, the inverse formalism separates them optimally to accurately estimate each of them in any given space–time location. And with regard to present satellite configurations (e.g., Geosat, *ERS-1*, Topex/Poseidon), the orbit error may be near optimally estimated from altimetry using the crossover points only. The whole process on the altimeter data is called the "crossover inverse method" (CIM). Our aim is to prove the value of this new method for correcting altimeter data from orbit error. It is used here in a restricted environment, for a limited geographic area (a few thousand kilometers wide). We extracted the variable oceanic signal from altimetry in the Brazil–Malvinas confluence area and compared it to the signal estimated using short-arc polynomial adjustments. The altimeter data was taken from the 17-day repeat orbit of the Geosat Exact Repeat Mission (Cheney et al. 1987). The area was chosen for its high level of energy and nonhomogeneity. It is also a very interesting area for the dynamics and is being thoroughly investigated by international World Ocean Circulation Experiment (WOCE) teams (Confluence Principal Investigators 1990).

Sections 2 and 3 discuss the principles of the CIM: section 2 summarizes the formalism; section 3 describes the altimeter data subset, that is, the crossover points and statistics of the altimeter signal. Section 4 presents results that formally validate the use of the crossover point subsampling to correct altimeter data for orbit error. Section 5 shows how important it is to realistically describe, in terms of statistics, the orbit error signal (variability level, decorrelation period) and the variable oceanic signal (variability level, nonhomogeneities). Section 6 compares two types of eddy fields computed at an arbitrary date in the confluence area: first, with this new approach and, second, using a conventional short-arc polynomial method. Section 7 provides the main conclusions and possible enhancements of the method.

2. The crossover inverse method

Correction of the altimeter signal for orbit error is best achieved by a form of optimal analysis known as the inverse formalism (Wunsch and Zlotnicki 1984; Mazzega and Houry 1989). A major difficulty is to describe the orbit error spectrum realistically. If we refer altimeter profiles to the mean profile, we remove the mean sea level signal as well as the gravitational part of the orbit error, which is the part due to the gravity field, the least known component. The altimeter residuals reveal three components: the variable orbit error, the variable oceanic signal, and the altimeter noise.

The optimal method would use all altimeter residual data to estimate the oceanic variability or the orbit error in a single operation (matrix inversion). It would require a correspondingly large computational effort—hence, problems of memory size, system stability, and CPU time. As our aim is to estimate the oceanic variability, which is to correct the variable altimeter signal

for the variable orbit error, we suboptimize the method relying mainly on the fact that the variable orbit error is a long-wavelength signal. We used the inverse formalism to estimate the variable orbit error P and the associated covariance errors $\mathbf{C}_P$, limiting the altimeter data in space to the profile altimetric information sampled at the crossover points, that is, where the profiles meet other profiles (intersections of ascending and descending ground tracks). For present satellite configurations (e.g., Geosat, *ERS-1*, Topex/Poseidon), the along-track distance between two time-successive crossover points varies from a few kilometers at high latitudes to 100 km at the equator. To further reduce the number of data points, we confined the altimeter data to the geographic area we studied (a few thousand kilometers wide).

The following are detailed formulas:

$$P(r_k, t_k) = \sum_{i=1}^{\mathrm{Nda}} C_0(r_k, t_k; r_i, t_i) \sum_{j=1}^{\mathrm{Nda}} (\mathbf{S}^{-1})^{ij} \mathrm{da}^j(r_j, t_j), \quad (1)$$

$$C_P(r_k, t_k; r_{k'}, t_{k'}) = C_0(r_k, t_k; r_{k'}, t_{k'}) - \sum_{i=1}^{\mathrm{Nda}} C_0(r_k, t_k; r_i, t_i) \times \sum_{j=1}^{\mathrm{Nda}} (\mathbf{S}^{-1})^{ij} C_0(r_j, t_j; r_{k'}, t_{k'}), \quad (2)$$

where

- i is a crossover point (id., j and k),
- (r_i, t_i) are the space and time coordinates of the crossover point i (id., j and k),
- da^j is the residual altimeter measurement at the crossover point j,
- Nda is the number of altimeter data or crossover points,
- $\mathbf{S}$ is the covariance matrix describing all residual altimeter signal components ($\mathbf{S} = \mathbf{C}_0 + \mathbf{C}_{\mathrm{da}}$)
- $\mathbf{C}_0$ is the covariance model describing the orbit error signal to estimate (a priori),
- $\mathbf{C}_{\mathrm{da}}$ is the covariance matrix describing the residual altimeter signal components except the one to be extracted (oceanic variability and altimeter noise) (a priori),
- P is the inverse estimate of the variable orbit error signal (a posteriori), and
- $\mathbf{C}_P$ is an error estimate on P, that is, the error covariance (a posteriori). (It is computed for points k' surrounding the crossover point k.)

The rms error on the P estimate of the crossover point k is simply given by $[C_P(r_k, t_k; r_k, t_k)]^{1/2}$.

The inverse solution will remain quasi-optimal if we used the right a priori covariance functions (see the weight matrix $\mathbf{S}$). The covariance functions describe the statistical behavior of all altimeter components. They are defined in section 3. The whole a priori information ensures the stability of the equations and uniqueness of the solution.

We then estimate the variable orbit error for any altimeter data by means of a weighted linear interpolation scheme applied to orbit error values and their a posteriori errors of the two crossover points that surround the data (proximity in time).

3. The altimeter data

The altimeter data are from the 8 November 1986–8 November 1988 Geosat Exact Repeat Mission (ERM). They correspond to the first 43, 17-day repeat cycles. The sea surface height measurements (SSH) are obtained using ephemeris computed at Goddard Space Flight Center with the GEM-T2 earth gravity field and referenced to the 1980 Geodetic Reference System ellipsoid (GRS80). The altimeter data were first edited in the Brazil–Malvinas confluence area (47°–34°S, 62°–43°W) and validated. SSHs are corrected for the following effects (corrections available in the GDRs): electromagnetic bias by adding 2% of significant wave height, ocean tides using the Schwiderski model (Schwiderski 1980), terrestrial tides using the Cartwright model (Cartwright and Tayler 1971), ionospheric effects using the Global Positioning System (GPS) climatic model, and dry and wet tropospheric effects using Fleet Numerical Oceanography Center (FNOC) data (Cheney et al. 1987). Because of the uncertainties of estimating an inverted barometer correction (see Zlotnicki et al. 1989), none was applied. The once per second original sampling is then changed into 10-km along-track sampling to align the data on a fixed latitude grid (using a cubic spline interpolation), and each individual profile is referred to the mean profile. The mean profile is computed by averaging together only complete repeat profiles (about 80% of the profiles). The mean profile consists of the geoid, the time-invariant dynamic topography, and the mean errors—that is, the gravitational part of the orbit error and the mean of remaining errors after corrections—whereas residuals reveal the sea surface variability signal as well as unremoved errors (mainly the nonsystematic orbit error). Because of the orbit error field, an external mean sea level signal would be of no use.

The final set of crossover points is obtained, track by track, by linear interpolation between the two residual altimeter data points surrounding each crossover point and separated in time by no more than 2 s. To avoid aliasing and reduce noise, residual altimeter profiles need to be filtered before subsampling. We used a Lanczos filter (Hamming 1977) with a cutoff wavelength set to 200 km (approximately twice the distance between two crossover points).

The residual altimeter data reveal three components: the variable orbit error, the variable oceanic signal, and

the altimeter noise. Each one needs describing in terms of covariance functions that are defined from the space lag D and the time lag T between any pair i and j of altimeter data points at space–time coordinates r_i, t_i and r_j, t_j, respectively.

• Orbit error—the major source of altimetric errors—known also as "satellite radial position error," is the difference between the true orbit and the calculated orbit. Since it applies to residual altimeter data, this error concerns the variable part or the nongravitational part of the total orbit error. For each orbit integration arc, we used a method similar to Houry et al. (1994) on the residual altimeter data to determine the residual orbit error frequency spectrum, its time validation period, as well as its constants. The spectrum is relatively simple (no gravity effects) (see Chelton and Schlax 1992) and characterized by a prominent peak at the once per orbital revolution frequency (1/Trev) (Fig. 1). A simple analytical model of the covariance function D1 is a cosine at 1/Trev damped by an exponential decay (DT) (Wunsch and Zlotnicki 1984): for example,

$$\mathrm{D1}(r_i, t_i; r_j, t_j) = \sigma_{\mathrm{orb}}^2 \cos\left(\frac{2\pi T}{\mathrm{Trev}}\right)\exp\left(-\frac{T^2}{\mathrm{DT}^2}\right). \quad (3)$$

The nominal radial accuracy σ_{orb} is 30 cm rms, and the decorrelation time (DT) is set to 30 orbital revolution periods (2.1 days). As the orbital calculation is reinitialized periodically, the correlation is set to zero between two measurements from different calculations, that is, belonging to different orbit integration arcs (which are 6 days long for the GEM-T2 orbit) (Mazzega 1986). The model is more sophisticated than other methods (see section 1), and points belonging to successive orbital revolutions are correlated.

• Variable oceanic signal (mesoscale). It is known from spectral analyses of Geosat altimeter measurements processed using the collinear-track method and short-arc polynomial adjustments (Provost and Le Traon 1992). We represented the space–time covariance function D2 by the isotropic space correlation function put forward by Arhan and Colin de Verdière (1985), multiplied by a Gaussian temporal decreasing function:

$$\mathrm{D2}(r_i, t_i; r_j, t_j) = \sigma_{\mathrm{var}}(r_i)\sigma_{\mathrm{var}}(r_j)\left(1 + R + \frac{R^2}{6} - \frac{R^3}{6}\right) \times \exp(-R)\exp\left(-\frac{T}{T_{\mathrm{var}}}\right) \quad (4)$$

with

$$R = D/R_{\mathrm{var}}. \quad (5)$$

The mean rms variability σ_{var} is about 15 cm rms, while the real rms values $\sigma_{\mathrm{var}}(r_i)$ and $\sigma_{\mathrm{var}}(r_j)$ are determined

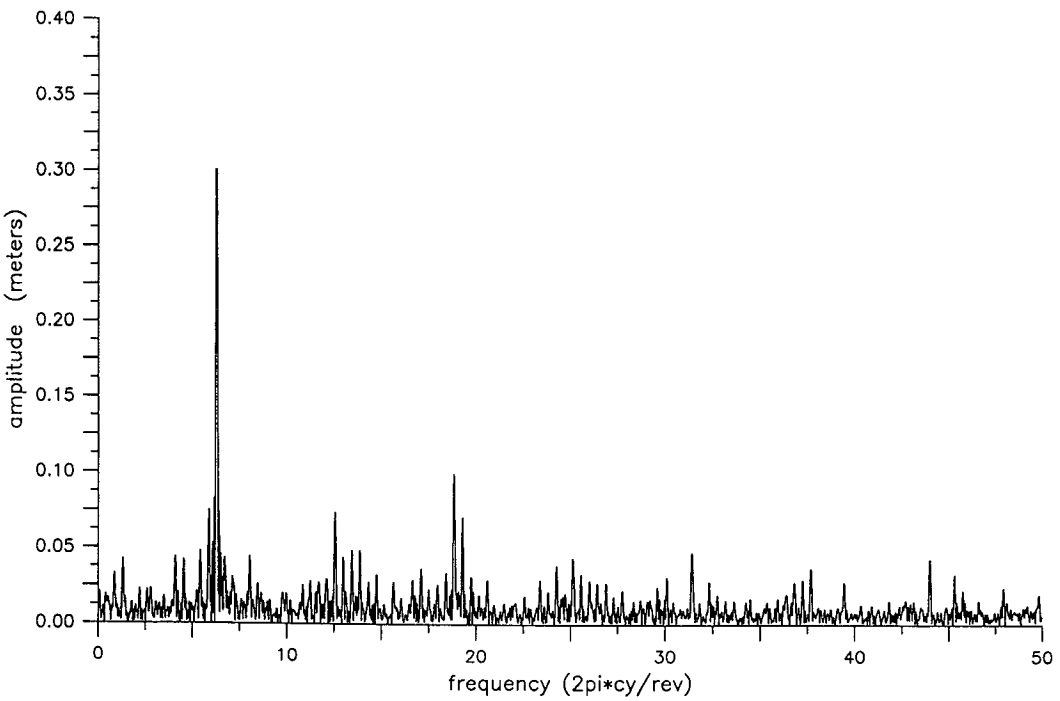

FIG. 1. Periodogram of the difference between Geosat ERM altimeter heights and the mean profiles calculated with the GEM-T2 gravity field for a 6-day arc. The spectrum is relatively simple and dominated by a once-per-revolution peak that is largely due to orbit errors.

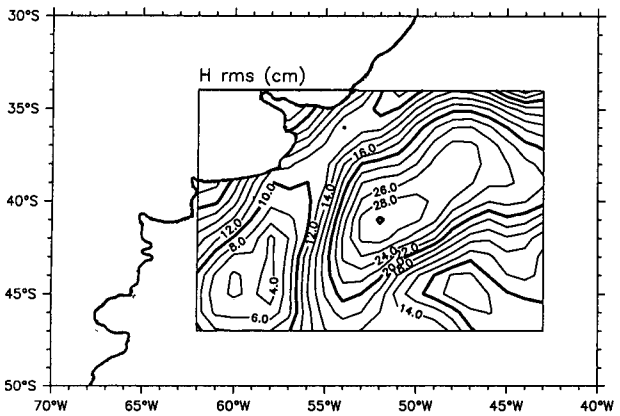

FIG. 2. Root-mean-square oceanic variability (cm rms) computed from the first 2 years of Geosat ERM altimeter data, using the short-arc collinear-track method. Objective analysis was applied to filter out small-scale features.

on $2° \times 2°$ boxes (Fig. 2). Spatial and temporal scales R_{var} and T_{var} are taken, respectively, as 54 km and 20 days.

Prior filtering of the altimeter data removes some of the oceanic signal but the amount removed is less than 10% of the signal variance and does not significantly affect the statistics discussed above. If any more is removed, the variance could be modified.

- Altimeter instrument noise, treated as white noise. The covariance function D3 is modeled by a Dirac delta:

$$\mathrm{D3}(r_i, t_i; r_j, t_j) = \sigma^2_{\text{alt}}\delta(T). \quad (6)$$

Geosat altimeter noise σ_{alt} is 3–4 cm rms for the 1-s average. However, it is clear that filtering considerably reduces the altimeter noise level, and we therefore chose a value of 2 cm rms.

- The complete data error covariances $\mathbf{C}_0$, $\mathbf{C}_{\text{da}}$, and $\mathbf{S}$ (see section 2) are defined as follows:

$$C_0(r_i, t_i; r_j, t_j) = \mathrm{D1}(r_i, t_i; r_j, t_j), \quad (7)$$

$$C_{\text{da}}(r_i, t_i; r_j, t_j) = \mathrm{D2}(r_i, t_i; r_j, t_j) + \mathrm{D3}(r_i, t_i; r_j, t_j), \quad (8)$$

$$S^{ij} = C_{\text{da}}(r_i, t_i; r_j, t_j) + C_0(r_i, t_i; r_j, t_j). \quad (9)$$

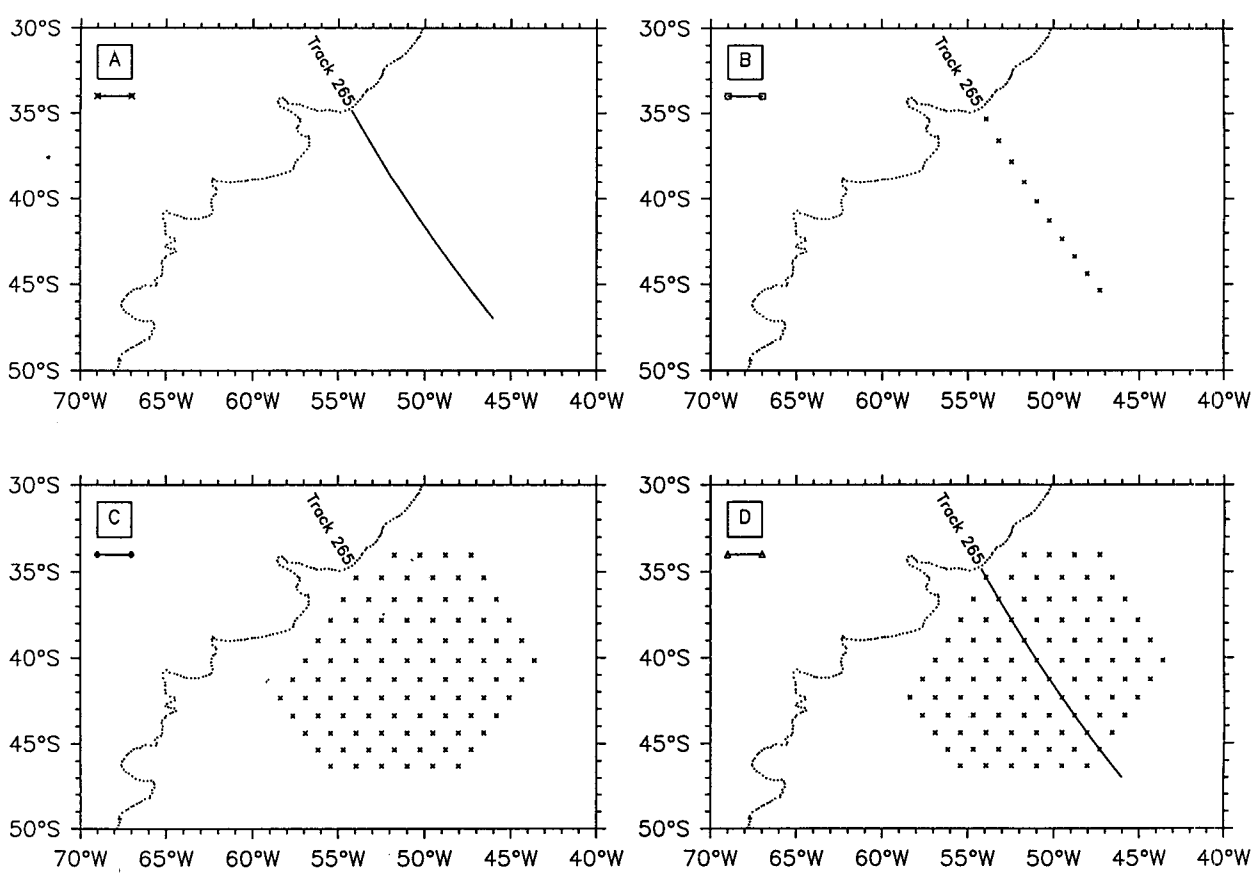

FIG. 3. Four Geosat altimeter subsamplings showing the importance of crossover points in the inverse formalism. Case A is a 1500-km altimeter profile sampled every 10 km (track 265, cycle 3). Case B is the same profile sampled at crossover points. Case C is the crossover points in the confluence area. Case D is cases A and C together, all the crossover points, and the altimeter profile residuals.

As the radial orbit error is decorrelated from one integration arc to the next, we split the single dataset into integration arcs. To constrain the inverse formalism satisfactorily, that is, to make it easier to separate the orbit error signal and the variable oceanic signal, we surrounded each arc with 20 days of altimeter crossover points. Each final dataset covers a 46-day period for a 6-day period estimate. They contain 1000–1500 data points and can be handled by the inverse formalism in one hour's CPU time on a workstation such as a Sun Sparc 1.

4. Validating the crossover point subsampling

To test the importance of the crossover point information to separate the altimeter signal components, that is, the orbit error and the oceanic variability, we applied the inverse formalism four times to estimate the a posteriori orbit error variance (called below a posteriori error) along one altimeter profile, using different altimeter datasets (Fig. 3). The altimeter profile is selected arbitrarily. It corresponds to track 265 of cycle 3. It is 1500 km long and located in the confluence area. The four altimeter datasets contain altimeter measurements made during a 66-day period centered on the profile date. The first set (case A) contains the altimeter profile residuals. The second set (case B) contains the crossover points of the profile. The third set (case C) contains all crossover points in the confluence area. The fourth set (case D) represents cases A and C together, which is all the crossover points plus the altimeter profile residuals. To illustrate a general case and really understand the influence of the crossover points, we considered the nominal error on the variable oceanic signal to be homogeneous and equal to 15 cm rms.

Figure 4 shows the a posteriori along-track error. With only the altimetric information from the profile, the a posteriori errors are minimum at the center of the profile (about 5 cm rms) and a little higher at its edges (about 5.5 cm rms). The orbit error estimate is less constrained at its edges. With the complete crossover point information (cases C and D), the a posteriori errors are identical all along the altimeter profile and equal to 2 cm rms. Using the complete crossover point information instead of the along-track altimetric information avoids edge effects and more than doubles accuracy. Comparing case A with case B or case C with case D, illustrates that subsampling the altimeter profile at the crossover points only slightly degrades the final solution: the a posteriori errors are very similar. We also computed the a posteriori error using a conventional short-arc polynomial adjustment, the least-squares fit method (LSF) and compared it with the errors of cases A or B. Profiles have a similar shape, minimum at the center and maximum at the edges. The values at the center are nearly equal, whereas the values at the edges differ, being much higher for the

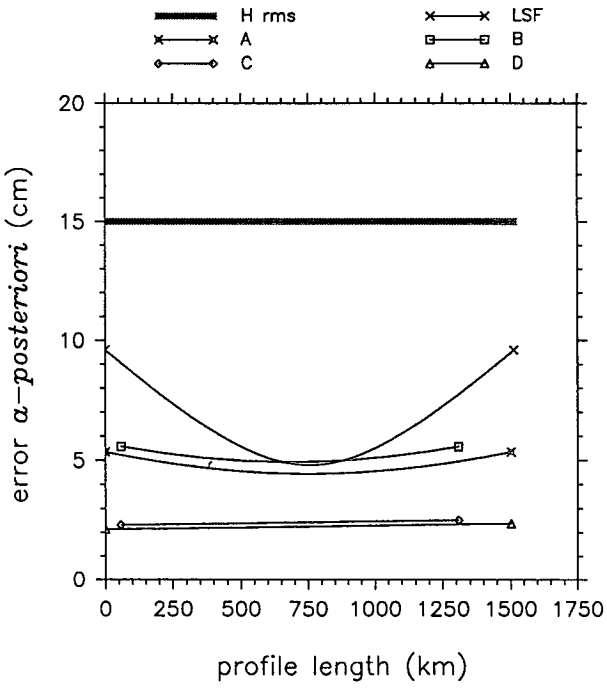

FIG. 4. A posteriori errors (cm rms) on the orbit error estimated along track 265 of cycle 3, using the inverse formalism and subsamplings A–D (see Fig. 3). LSF is the error a posteriori on the orbit error estimation using the LSF method. The variability of the mesoscale signal (*H* rms) is assumed to be homogeneous and equal to 15 cm rms.

LSF method (9.5 cm rms). The differences are because the LSF method fits a zero- or one-degree polynomial to the profile with no prior knowledge, while the inverse method uses the statistical a priori information on the orbit error, oceanic variability, and altimeter noise (e.g., variance terms). More comments are given in Le Traon et al. (1991). The main conclusion of the test shown in Fig. 4 is that by using only the altimetric information at crossover points, the method remains nearly optimal.

Due to the signal spectrum characteristics, the orbit error is better determined from altimetry in low-variability areas (better signal-to-noise ratio) and less well determined in high-variability areas. The confluence area is known to be a high-variability area. We thought this feature could help us decorrelate the signals better. It is certainly feasible as far as the satellite track geometry and orbit error spectrum characteristics were concerned. [The orbit error spectrum characteristics are a function of time over 30 orbital revolutions or 2.1 days (see section 3).] Indeed, two altimeter data points separated by a satellite revolution and belonging to the same integration arc are still correlated in terms of the orbit error. With the Geosat satellite, the two points are at the same latitude but 25°25′ farther west or east, and thus uncorrelated in terms of the variable signal. This can be extended to a whole area. For the confluence area, the other area is identical in size and

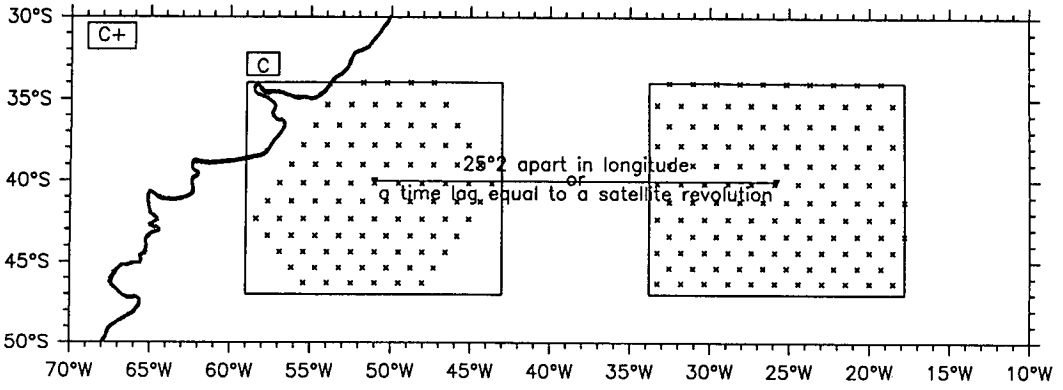

FIG. 5. Case C+ summarizes altimeter subsamplings in the confluence domain (see Fig. 3, case C) and a prao area. A prao area is a domain similar to confluence but separated in time by one satellite orbital revolution period. For Geosat, it is at the same latitude and 25°25′ farther west or east. At 25°25′ farther east, we have a fairly homogeneous low-energy area in contrast with the high-variability confluence area.

25°25′ farther west or east. At 25°25′ farther east, we have a fairly homogeneous low-energy area. By adding the altimetric information at its crossover points to the confluence altimetric information into the inverse formalism (see Fig. 5), we reduced the a posteriori error from 2.4 to 1.6 cm rms along the above profile (Fig. 6), thus improving the orbit error estimate. The second dataset acts like a counterweight. We called it the "prao contribution." (Note: A prao is a Malayan boat made of two bodies, a central part plus a pendulum.)

5. Sensitivity to a priori statistical description

The inverse formalism needs a realistic statistical description of each term it uses, that is, mainly the orbit error and oceanic variability. In this section, we tested the sensitivity of the method to three major statistical parameters: orbit error decorrelation time, orbit error variance, and oceanic signal variance. (The other parameters are those described in section 3.) We varied these parameters one at a time. Nominal values are set to 30 orbital revolutions (2.1 days), 30 and 15 cm rms. Note again that to illustrate a general case and really understand the influence of each variable, we considered the oceanic signal variance to be homogeneous. The altimeter dataset is case C. The orbit error is estimated along the profile of section 4. For each sensitivity case, we compared the a posteriori rms errors (Figs. 7a–c):

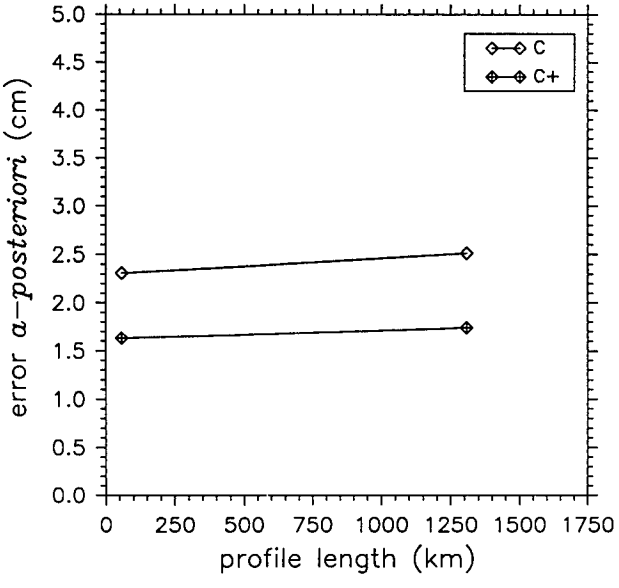

FIG. 6. A posteriori errors on the orbit error estimated along track 265 of cycle 3, using the inverse formalism and subsamplings C and C+ (see Fig. 5). The prao contribution improves the orbit error accuracy from 2.4 to 1.6 cm rms.

- A shorter orbit error decorrelation period such as 10 orbital revolutions (0.7 days) mainly increases the error a posteriori at the profile edges: the problem becomes less constrained as for polynomial adjustment. On the other hand, a maximum value—because of integration arcs—such as 100 orbital revolutions (7 days) reduced it by 0.2 cm equally along the profile (no edge effects).
- The higher the orbit error variance, the less accurately the orbit error is estimated. The effects are greater at the edges. However, the differences in variance depend on the orbit error decorrelation period and are considerably weaker at or above 30 orbital revolutions.
- As expected, a factor of 2 in the a priori oceanic signal variance affects the accuracy of the orbit error estimation equally along the altimeter profile.

Sensitivity to the a priori orbit error signal has shown that with the above scales (see section 3 for justification) the problem is well constrained and a small perturbation on one scale does not change the results drastically. Sensitivity to the a priori oceanic variability confirms an established fact: the method needs a re-

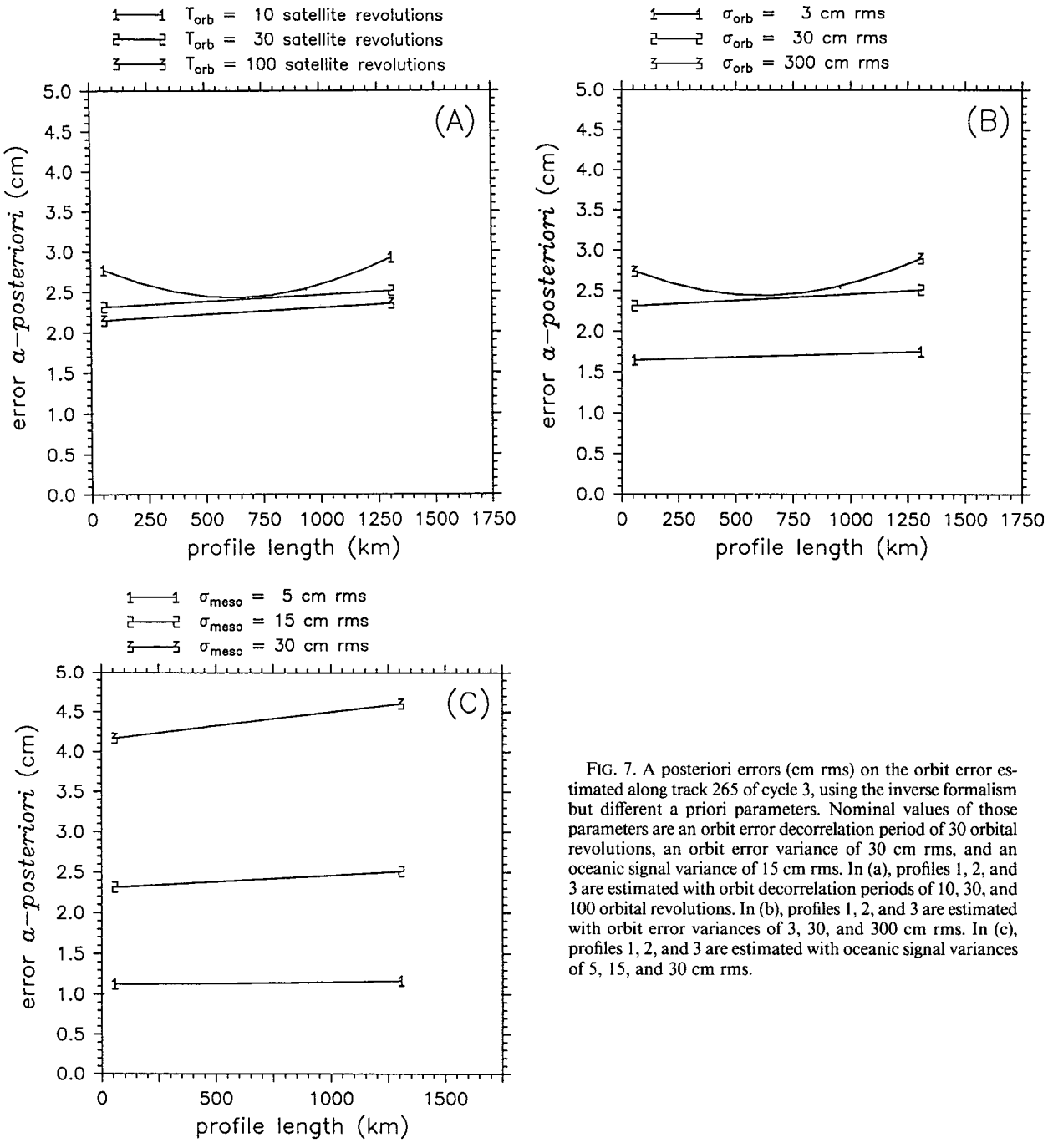

FIG. 7. A posteriori errors (cm rms) on the orbit error estimated along track 265 of cycle 3, using the inverse formalism but different a priori parameters. Nominal values of those parameters are an orbit error decorrelation period of 30 orbital revolutions, an orbit error variance of 30 cm rms, and an oceanic signal variance of 15 cm rms. In (a), profiles 1, 2, and 3 are estimated with orbit decorrelation periods of 10, 30, and 100 orbital revolutions. In (b), profiles 1, 2, and 3 are estimated with orbit error variances of 3, 30, and 300 cm rms. In (c), profiles 1, 2, and 3 are estimated with oceanic signal variances of 5, 15, and 30 cm rms.

alistic description of this signal in terms of energy level or variance.

6. Application

In this section, we used the CIM to correct for orbit error 2 years of Geosat data in the confluence area. The a priori altimeter dataset is the subsampling of the altimeter data at crossover points. The oceanic variability is no longer assumed to be homogeneous since the confluence area is highly variable (see Fig. 2 and section 3). To handle the altimeter data on our Sun workstation, we restricted ourselves to 1000–1500 data points per run. Therefore, we decided not to use the prao contribution. Also, to avoid boundary effects, the signal is estimated in an inner domain, 2° smaller in latitude and longitude (i.e., 1° from the boundaries).

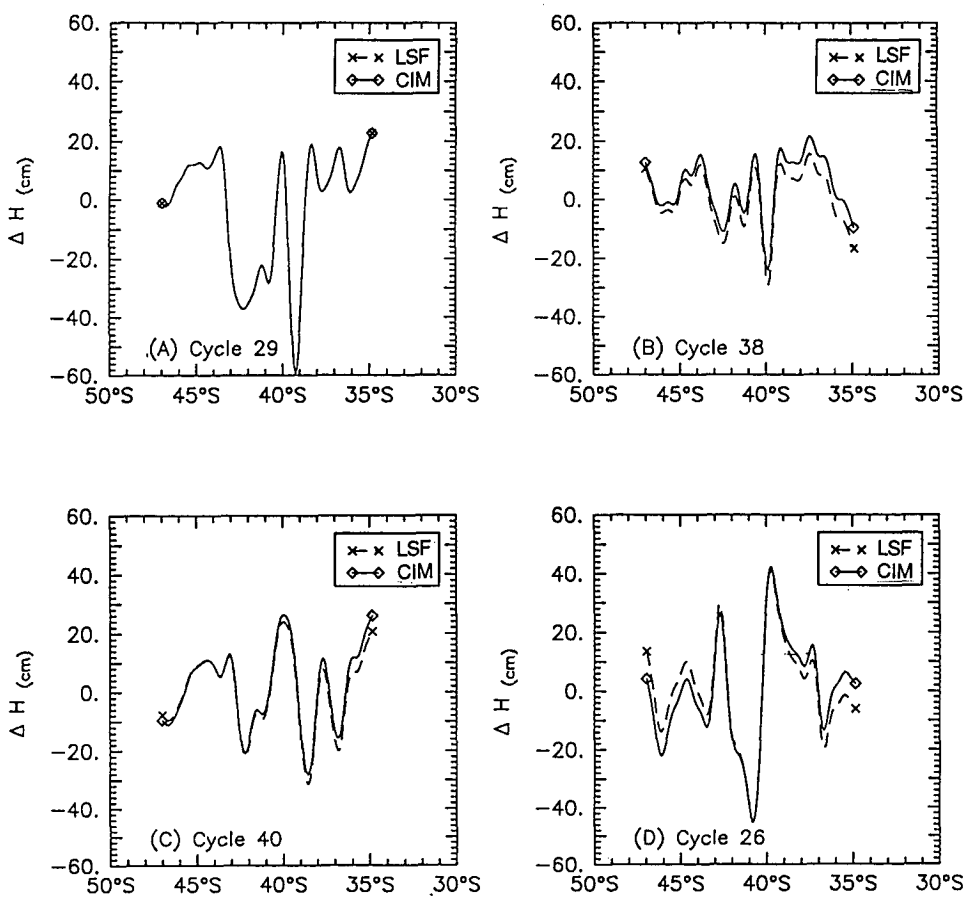

FIG. 8. Residual altimeter profiles (cm) of track 265 of cycles (a) 29, (b) 38, (c) 40, and (d) 26, corrected for orbit error using either the CIM (plain line) or the LSF (dashed line).

To validate the orbit error reduction, we investigated a few items:

1) rms of altimeter residual crossover differences (CROSSRMS),
2) adjusted altimeter profiles, and
3) oceanic variability (rms).

1) CROSSRMS is computed using residual crossover differences in the confluence area and a time lag below a maximum absolute value. The CIM reduces CROSSRMS from 47 to 18 cm for a maximum absolute time lag of 17 days (the repeat period), and 47 to 14 cm for a maximum absolute time lag of 3 days. In both cases, the reduction is significant enough to validate the orbit error adjustment. Indeed, the rms value of 18 cm is comparable to the one obtained with a global constrained sinusoidal adjustment. Unlike the conventional crossover adjustment method, the CIM shows a correlation between the CROSSRMS and the time lag: the rms value decreases with it. Such correlation is expected because the oceanic signal in the confluence area is more and more decorrelated with time lag: at 10 days, half of the signal is already decorrelated (Provost and Le Traon 1993).

2) To highlight the effectiveness of the orbit error reduction method, we compared residual altimeter profiles adjusted with either the CIM or the LSF method. Results are similar for all tracks. In Fig. 8, we plotted four typical examples for track 265. Each example represents a cycle: the first (a) shows identical reduction, the second (b) a bias, the third (c) a very small bias, and the fourth (d) a bias at the edges. Biases are arbitrarily positive or negative. To summarize all cycles, we computed the along-track variability (rms) (see Fig. 9). The variability obtained with a CIM adjustment is similar to that with LSF but at a higher level. The difference (the small black boxes) never exceeds 6 cm rms and closely tracks the variance profile shape: local minima at local minima, local maxima at local maxima.

3) To see the total effect of the CIM adjustment in the confluence area, we computed the global variability (Fig. 10) and compared it to the a priori map (Fig. 2). The conclusions of the above paragraph remain valid: the variability is similar to the reference level though it increases by about 2 cm rms. Differences in the frontal area support use of the CIM, the oceanic variability being better estimated. Along-coast differences are quite

significant and we think they are due to a problem in tidal corrections. The CIM cannot overcome such problems, because of the a priori knowledge on altimeter errors (see section 3). As the LSF method acts as a high-pass filter, it corrects each altimeter profile for all the long-wavelength signals (with respect to the area size)—for example, orbit error, long-wavelength variable oceanic signal, residual tropospheric correction error, and residual tidal error.

7. Conclusions

Different conventional orbit reduction schemes affect the magnitude and spectral characteristics of the oceanic variability, with effects depending on the size of the experiment area. An optimal interpolation scheme can correct residual altimeter data for orbit error. Due to the space and time characteristics of the altimeter measurement errors (mainly orbit error and altimeter noise) and signal noise (i.e., oceanic variability), large quantities of data in extensive domains need analyzing at the same time. Therefore, and with regard to present satellite configurations (Geosat, *ERS-1*, Topex/Poseidon), we validated to reduce the whole set of altimeter data to the crossover points over limited areas (a few thousand kilometers wide). The data selection over a few 10-day periods is a consequence of the spectral characteristics of the signal components. The method is called the crossover inverse method (CIM). It has been tested in the confluence area with two years of the Geosat ERM. Analysis of the a posteriori error on the orbit error estimate proved the method to be quite effective. The rms value of residual crossovers is reduced from 47 to 14–18 cm, depending on time lag, and the oceanic variability is estimated at a level about 13% higher than with the conventional short-arc polynomial adjustment method.

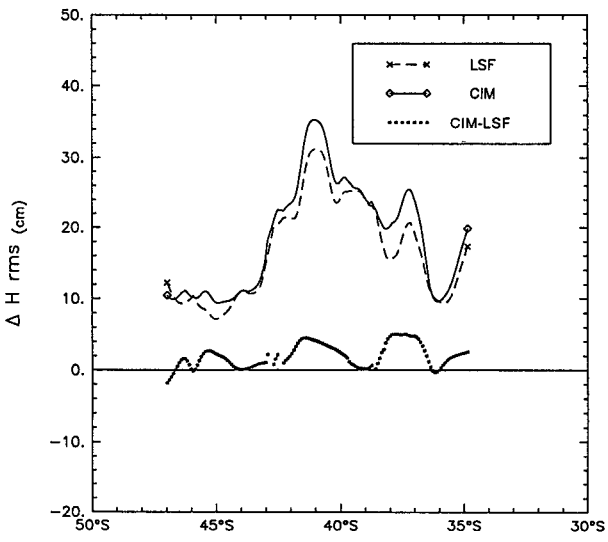

FIG. 9. Root-mean-square variability (cm rms) of altimeter profiles of track 265 (all cycles) corrected for orbit error using either the CIM (plain line) or the LSF method (dashed line). The small black boxes represent the difference between CIM and LSF.

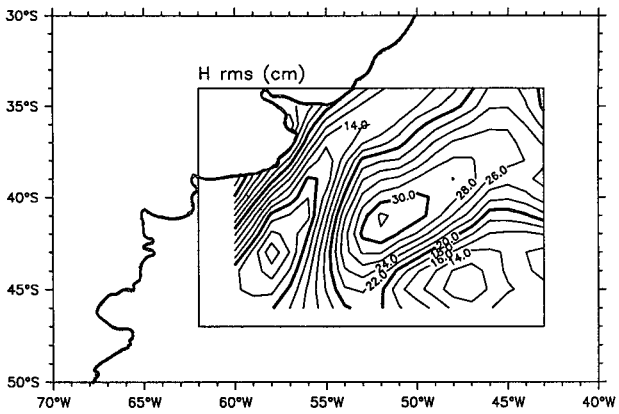

FIG. 10. Root-mean-square oceanic variability (cm rms) computed from the first 2 years of Geosat ERM altimeter data, using the CIM. Objective analysis filtered out small-scale features.

However, the effectiveness of the CIM depends strongly on three parameters:

1) the quality of repeated tracks so as to obtain a mean profile homogeneous from one track to the next,
2) a full, accurate statistical description of the altimeter signal components, and
3) the space and time selection of crossover points.

Since the Geosat repeat band measures 2 km, the first requirement is met by having a large number of complete repeat tracks so as to accurately estimate the mean track. The second requirement is more difficult to meet and the description may depend strongly on the experiment area. The application described above is an example of such a problem with the "residual" tidal signal. Actually, the problem may occur for all residual environmental corrections. With the Topex/Poseidon altimetric mission whose main goal is to observe large-scale oceanic variability, such residual errors would be lower. And the method presented here should therefore be very useful. The third and last requirement has been overcome with our restricted application case. It needs to be further investigated to adapt the method for a global process. We will then need to validate it, comparing the method to the best prevailing global method for orbit error estimation (e.g., the least-squares fits of sinusoids over long arcs)

Acknowledgments. We thank Nigel Greenwood for helping us correct the English style and clarity. This study was partly supported by a SHOM/CLS Contract 90-87-019-00.

REFERENCES

Arhan, M., and A. Colin de Verdière, 1985: Dynamics of eddy motions in the eastern North Atlantic. *J. Phys. Oceanogr.*, **15**, 153–170.

Cartwright, D. E., and R. J. Tayler, 1971: New computations of the tide generating potential. *Geophys. J. Roy. Soc.*, **23,** 45–74.

Chelton, D. B., and M. G. Schlax, 1993: Spectral characteristics of time-dependent orbit errors in altimeter height measurements. *J. Geophys. Res.*, **98,** 12 579–12 600.

——, M. G. Schlax, D. L. Witter, and J. G. Richman, 1990: Geosat altimeter observations of the surface circulation of the southern ocean. *J. Geophys. Res.*, **95,** 17 877–17 903.

Cheney, R. E., and L. Miller, 1990: Recovery of sea level signal in the western tropical Pacific from GEOSAT altimetry. *J. Geophys. Res.*, **95,** 2977–2984.

——, J. G. Marsh, and B. D. Beckley, 1983: Global mesoscale variability from collinear tracks of SEASAT altimeter data. *J. Geophys. Res.*, **88,** 4343–4354.

——, B. C. Douglas, R. W. Agreen, L. Miller, D. L. Porter, and N. S. Doyle, 1987: NOAA GEOSAT altimeter geophysical data record user handbook. NOAA Tech. Memo., NOS NGS-46, 28 pp.

——, B. C. Douglas, and L. Miller, 1989: Evaluation of GEOSAT altimeter data with application to tropical Pacific sea level variability. *J. Geophys. Res.*, **94,** 4737–4747.

Confluence Principal Investigators, 1990: An intensive study of the southwestern Atlantic. *EOS Trans.*, **71,** 1131–1133.

Douglas, B. C., D. C. Mc Adoo, and R. E. Cheney, 1987: Oceanographic and geophysical applications of satellite altimetry. *Rev. Geophys.*, **25,** 875–880.

Fu, L. L., and D. B. Chelton, 1985: Observing large scale temporal variability of ocean currents by satellite altimetry: With application to the Antarctic circumpolar current. *J. Geophys. Res.*, **90,** 4721–4739.

Hamming, R. W., 1977: Digital filters. *Signal Processing,* A. V. Oppenheim, Ed., Prentice Hall.

Houry, S., J. F. Minster, C. Brossier, K. Dominh, M. C. Gennero, A. Cazenave, and P. Vincent, 1994: Radial orbit error reduction and mean sea surface computation from the Geosat altimeter data. *J. Geophys. Res.*, in press.

Le Traon, P. Y., C. Boissier, and P. Gaspar, 1991: Analysis of errors due to polynomial adjustment of altimeter profiles. *J. Atmos. Oceanic Technol.*, **8,** 385–396.

Marsh, J. G., T. V. Martin, 1982: The Seasat altimeter mean sea surface model. *J. Geophys. Res.*, **87,** 3269–3280.

Mazzega, P., 1986: How radial orbit errors are mapped in altimetric surfaces. *J. Geophys. Res.*, **91,** 6609–6628.

——, and S. Houry, 1989: An experiment to invert Seasat altimetry for the Mediterranean and Black Sea mean surfaces. *Geophys. J.*, **96,** 259–272.

Ménard, Y., 1983: Observation of eddy fields in the northwest Atlantic and northwest Pacific by Seasat altimeter data. *J. Geophys. Res.*, **88,** 1853–1866.

Provost, C., and P. Y. Le Traon, 1993: Spatial and temporal scales in altimetric variable in the Brazil–Malvinas current confluence region: Dominance of the semi-annual period and large scales. *J. Geophys. Res.*, **98,** 18 037–18 051.

Sandwell, D. T., and B. Zangh, 1989: Global mesoscale variability from the GEOSAT Exact Repeat Mission: Correlation with ocean depth. *J. Geophys. Res.*, **94,** 17 971–17 984.

Schwiderski, E. W., 1980: On charting global tides. *Rev. Geophys. Space Geophys.*, **18,** 243–268.

Tai, C. K.: 1988, Geosat crossover analysis in the tropical Pacific. 1: Constrained sinusoidal crossover adjustment. *J. Geophys. Res.*, **93,** 10 621–10 629.

——, 1989: Accuracy assessment of widely used orbit error approximations in satellite altimetry. *J. Atmos. Oceanic Technol.*, **6,** 147–150.

——, 1991: How to observe the gyre to global scale variability in satellite altimetry: Signal attenuation by orbit error removal. *J. Atmos. Oceanic Technol.*, **8,** 271–288.

——, and L. L. Fu, 1986: On crossover adjustment in satellite altimetry and its oceanographic implications. *J. Geophys. Res.*, **91,** 2549–2554.

Tarantola, A., and B. Valette, 1982: Generalized non linear inverse problems solved using the least squares criterion. *Rev. Geophys.*, **20,** 219–232.

Van Gysen, H., R. Coleman, R. Morrow, B. Hirsch, and C. Rizos, 1992: Analysis of collinear passes of satellite altimeter data. *J. Geophys. Res.*, **97,** 2265–2277.

Wagner, C. A., R. E. Cheney, 1992: Global sea level change from satellite altimetry. *J. Geophys. Res.*, **97,** 15 607–15 615.

Wunsch, C., and V. Zlotnicki, 1984: The accuracy of altimetric surfaces. *Geophys. J. Roy. Astron. Soc.*, **78,** 795–808.

Zlotnicki, V., L. L. Fu, and W. Patzert, 1989: Seasonal variability in global sea level observed with Geosat altimetry. *J. Geophys. Res.*, **94,** 17 959–17 969.